Ab initio calculation of time-dependent control dynamics in polyelectronic systems involving bound and resonance states: Application to a quartet spectrum of He^-

Yannis Komninos,[1,*] Theodoros Mercouris,[1,†] and Cleanthes A. Nicolaides[1,2,‡]
[1]*Theoretical and Physical Chemistry Institute, National Hellenic Research Foundation, 48 Vasileos Constantinou Avenue, Athens, 11635, Greece*
[2]*Physics Department, National Technical University, Athens, 15780, Greece*
(Received 25 October 2007; published 29 January 2008)

Using a pump-probe scheme with controllable time-delay in the range of 0–73 fs, we have solved from first principles the time-dependent Schrödinger equation (TDSE) describing a hyper-fast excitation process that involves both the discrete and the continuous spectrum of the three-electron atomic negative ion, He^-. Two approaches were implemented, both using state-specific wave functions for two multiply excited discrete states (the initial state, He^- $1s2s2p\ ^4P^o$, and the final state, He^- $2p^3\ ^4S^o$), and one intermediate state which is a shape resonance (He^- $1s2p^2\ ^4P$, including the underlying continuum of scattering states. The wavelengths of the two pulses connecting resonantly the states are in the infrared (10 080 Å) and in the soft x-ray region (323 Å). The first approach is analytic and solves the TDSE to first order in perturbation theory. This is acceptable for weak pulses whose duration is of the order of a few tens of femtoseconds. The second approach solves the TDSE nonperturbatively, via the state-specific expansion approach. A series of computations have produced time-dependent probabilities for preparing the triply excited bound state $He^-2p^3\ ^4S^o$ for various combinations of the duration of the two pulses. Apart from providing the first such quantitative data, the results suggest the appearance of effects of short-time nonexponential decay of resonances when it becomes possible to monitor excitation with time-delayed short pulses.

DOI: 10.1103/PhysRevA.77.013412 PACS number(s): 37.10.Jk, 32.80.Zb, 31.15.vj, 42.65.Re

I. INTRODUCTION

Given the possibility of experimenting with the interaction of electromagnetic pulses of various types with atoms and molecules, it is of interest to acquire reliable and quantitative information on related physically significant quantities. One type of theoretical approach to this problem has been, over a few decades, to employ models and obtain results on phenomenology. For example, various formalisms of time-dependent phenomena refer to model Hamiltonians for two- or multi-level atoms (molecules) interacting with one or more monochromatic beams of radiation, e.g., [1] and references therein. Some of the normally used related concepts are those of *Rabi frequencies*, of *detuning*, and of the *rotating wave approximation*.

On the other hand, it is natural to ask at a level beyond phenomenology about the time-dependent physics of atom–field interactions when real electronic structures and discrete as well as continuous spectra are considered. In this case, the computation from first principles for polyelectronic atoms is a much less developed area of research, with many unexplored areas.

A basic reason for this considerable lag is that, in such cases, the formulation of the *time-dependent many-electron problems* (TDMEPs) and the requirements for their quantitative solution must engage formalism and methodologies that not only are relevant but that may also lead in a practical way to physically transparent and reliable solutions of the polyelectronic *time-dependent Schrödinger equation* (TDSE). However, as it is easily appreciated, the solution of the polyelectronic TDSE from first principles, which is really what is needed if the physics of time-resolved dynamics in real atoms is to be understood quantitatively beyond phenomenology, is a much more complex enterprise than the solution of model problems. Needless to say, if one can solve the TDSE from first principles, then concepts of control for real systems, via the appropriate design of pulses and of excitation schemes, may be investigated rather reliably and realistically.

The time-dependent problems of quantum mechanics are normally treated, formally and computationally, in the framework of time-dependent perturbation theory. In this context, the usual computational approach is to assume that the perturbation is sufficiently weak so as to allow the truncation of the series of expansion of the time dependent wave function to first or, in certain cases, to second order. Of course, when the interaction is stronger, such an approach is inadequate. In such cases, the TDSE must be solved to all orders, or, practically speaking, directly and nonperturbatively.

A methodology for solving the TDSE nonperturbatively in atomic and small molecular systems was published some time ago under the name "state-specific expansion approach" (SSEA) [2,3]. The point of view that is expressed via the SSEA is that TDMEPs such as those connected to atom (molecule)-electromagnetic pulse interaction can be solved systematically by following the elegant and fundamental quantum mechanical concept of expansion of the time-dependent wave function over the unperturbed system's stationary states.

The key idea, apart from the necessary techniques developed for integrating the TDSE, is to capitalize on the knowl-

*ykomn@eie.gr
†thmerc@eie.gr
‡caan@eie.gr

edge and experience of computing and analyzing *state-specific* nonrelativistic or relativistic wave functions for electronic ground and excited stationary states by treating each time-dependent problem of interest in terms of expansions over such wave functions. For atoms, such an expansion has the form

$$\Psi_{SSEA}(t) = \sum_n c_n(t)\Phi_n(q) + \int_0 dE c_E(t)U_E(q',r). \quad (1)$$

The $\Phi_n(q)$ are N-electron state-specific square-integrable wave functions representing the discrete states and the localized components of the innerhole or multiply excited resonance states, and the U_E are N-electron scattering wave functions, energy normalized to $\delta(E-E')$. The symbols q,q' stand collectively for the coordinates of electrons in the bound orbitals of Φ_n and of U_E. The symbol r stands for the coordinates of the free electron(s) in U_E.

Since each term of Eq. (1) is supposed to be optimized in direct correspondence with the states of the spectrum of the unperturbed system, it is expected that a properly chosen expansion will be economical as well as physically transparent. Its substitution into the TDSE produces the corresponding coupled integrodifferential equations, whose solution under specified initial conditions (we have introduced a Taylor series technique [2]), produces the time-dependent coefficients as state-specific probability amplitudes. Convergence of the computation is tested by varying the total number of the states in Eq. (1), especially with respect to the range and density of the energy-discretized continuum.

The work reported here dealt with the *ab initio* solution of a time-dependent problem of control dynamics as a function of the time delay of two electromagnetic pulses of various durations, having wavelengths in the infrared region (10 080 Å) and in the soft x-ray region (323 Å) and interacting with excited electronic structures and scattering continua of the three-electron atomic negative ion (ANI), namely He^-. Specifically, the prototypical problem that was solved was formulated as follows: If one starts with the easily produced metastable state of He^-, the $1s2s2p\ ^4P^o$, and applies the aforementioned two pulses, how does the occupation probability of the final, triply excited bound state, the $He^-\ 2p^3\ ^4S^o$ (the target state), depend on time as a function of parameters of the interaction? In this context, the system of the physically relevant stationary states consists of two bound states and one shape resonance embedded in a single electron scattering continuum (Sec. II).

The relevant dynamics was investigated in two ways. In the first, it was obtained nonperturbatively, via the numerical solution of the TDSE by the implementation of the SSEA. In the second, the problem was solved at the level of first-order time-dependent perturbation theory (FOTDPT) via analytic methods. For weak fields, the two approaches yield the same numerical results. The analytic approach has the advantage of distinguishing the sources of the significant contributions to the evolution process.

II. CHOICE OF THE PHYSICAL SYSTEM

ANIs constitute a special class of species, for which experimental as well as theoretical interest has existed for many decades. A recent review by Andersen [4] on "*Atomic negative ions: Structure, dynamics and collisions*" contains an extensive discussion and cites 721 publications.

When reference to ANIs is made, one normally thinks of the stable ground state, if it exists. On the other hand, there is also plenty of interesting and challenging physics that is to be found in their excited states. These can be divided into two categories. The first consists of resonance ("compound") states with an intrinsic energy width caused by the mixing of bound with scattering components of the complete function space. In addition to [4], two review articles on such states, 20 years apart, have covered the subject since it started growing in the 1960s [5].

The second category of ANI excited states are the bound excited states, whose energy is sharp, e.g., [4,6,7] and references therein. By bound we mean that the state belongs to the nonrelativistic discrete spectrum and not that it is completely stable against radiative or relativistic nonradiative decay, unless of course its energy is below that of the ground state of the neutral atom. Obviously, as the effective nuclear charge increases across the Periodic Table, relativistic corrections as to the character of the spectrum must be considered. A short survey of known such states and an outline of a general computational methodology that allows the execution of accurate calculation and analysis on this subject was given 2 decades ago in [6]. The basic features of electronic structure that are responsible for their stability against nonrelativistic autoionization in spite of their high degree of excitation are discussed briefly in [7].

The measurement of properties of bound excited states of ANIs exhibits difficulties, of which a major one has to do with the preparation step. This is connected to the fact that, because these states have maximum spin multiplicities, the channels for their preparation and observation are limited.

The theoretical work whose results are presented here was conceived as a contribution not only to the theory and computation of control dynamics in general, but also to the quantitative understanding of the preparation of bound states of ANIs in the context of modern time-resolved spectroscopy.

Specifically, we have solved from first principles the TDSE, to first order as well as to all orders of perturbation theory, for the radiation-induced time-evolution over part of the spectrum of the three-electron He^-, consisting of one resonance and its scattering continuum, and two bound states. This time evolution is driven by two electromagnetic pulses with variable time overlap (i.e., pulse characteristics as well as time delay are control parameters), leading to the time-dependent occupation of the highest lying bound state of He^-, namely the $2p^3\ ^4S^o$.

The background on the relevant to the problem features of the He^- spectrum is the following.

Apart from its resonance spectrum, a portion of which has been studied over the years theoretically and experimentally, He^- also has a discrete spectrum that consists of two bound excited states, the $1s2s2p\ ^4P^o$ and the $2p^3\ ^4S^o$. In both cases, accounting for the large portion of the interelectronic interactions is crucial for establishing the above fact.

The existence of the metastable $1s2s2p\ ^4P^o$ state has been known for a long time [10–12] and was the early object of pioneering experimental studies on details of spectral prop-

erties [12,4]. As regards the $2p^3\,{}^4S^o$ state, its theoretically and computationally predicted existence and properties [8,9] were confirmed via subsequent additional calculations and via observations and analysis of beam-foil spectra [4,13]. Energy data for these two bound states from extensive computations of very high accuracy were published by Bylicki and Pestka [14]. They concluded that the $1s2s2p\,{}^4P^o$ state is 77.51 ± 0.04 meV below the He $1s2s\,{}^3S$ threshold, and that the $2p^3\,{}^4S^o$ state is 341.0 ± 0.1 meV below the He $2p^2\,{}^3P$ threshold. Accurate computation as well as experiment place the energy of the He $2p^2\,{}^3P$ bound state at 59.67 eV above the ground state [15].

One of the objects of the work in [9] was to determine quantitatively the probability of radiative transitions of the higher-lying $2p^3\,{}^4S^o$ state to the ${}^4P$ electron continuum above the He $1s2p\,{}^3P^o$ threshold, as determined by the amplitude $\langle 2p^3\,{}^4S^o|\vec{D}|1s2p\,{}^3P^o\varepsilon p\,{}^4P\rangle$, where $\vec{D}$ is the electric dipole vector operator and εp symbolizes the free electron. Inside this continuum there exist two multiply excited He^- states of ${}^4P$ symmetry, labeled by the $2s2p^2\,{}^4P$ and the $1s2p^2\,{}^4P$ configurations, which are also connected to the $2p^3\,{}^4S^o$ state via an electric dipole transition.

Given the spectrum of He, the $He^-\,2s2p^2\,{}^4P$ state is obviously autoionizing, lying inside one- and two-electron continua. The first accurate prediction of both its energy, $E = 57.42$ eV above the He ground state, and its total width, $\Gamma = 10.4$ meV, was presented in 1993 [16]. In 2004, its first observation, via photoabsorption from the metastable $1s2s2p\,{}^4P^o$, placed it at 37.668 ± 0.007 eV (i.e., 57.41 eV above the He $1s^2\,{}^1S$ state), with a width of 9.7 ± 0.2 meV [17]. It is thus confirmed that this resonance has a relatively narrow width. On the other hand, because of the small energy difference for the emission transition $He^-\,2p^3\,{}^4S^o \rightarrow 2s2p^2\,{}^4P$, which is only 1.91 eV, the $He^-\,2s2p^2\,{}^4P$ resonance does not contribute significantly to the total radiative emission cross section of the $2p^3\,{}^4S^o$ bound state, see Fig. 2 of [9(b)].

As regards the nature of the state labeled by the $He^-1s2p^2\,{}^4P$ configuration, this was uncertain until the systematic study of [9] demonstrated that it is a shape resonance and not a bound state, lying about 10 meV above the He $1s2p\,{}^3P^o$ threshold with a narrow width. Indeed, it was shown that this state manifests itself as a huge peak upon the radiative autodetachment of the $2p^3\,{}^4S^o$ state. The same intrinsic features of this shape resonance were established at about the same time by Hazi and Reed [18], who reported calculations of photoabsorption cross-sections with $1s2s2p\,{}^4P^o$ as the initial state. An accurate measurement of the energy, E, and width, Γ, of this state was reported in 1994 by Walter, Seifert, and Peterson [19], following their photodetachment experiments. They found that $E = 10.80 \pm 0.07$ meV above the He $1s2p\,{}^3P^o$ threshold and $\Gamma = 7.16 \pm 0.07$ meV.

Figure 1 depicts the information given above. It includes the relevant quartet states of He^- ($1s2s2p\,{}^4P^o$, $1s2p^2\,{}^4P$, and $2p^3\,{}^4S^o$), and the corresponding triplet states of He. For the two resonance states, $1s2p^2\,{}^4P$ and $2s2p^2\,{}^4P$, we have also written the values of their radiationless widths. Other possible He^-resonance states do not play a role in the problem that is considered here.

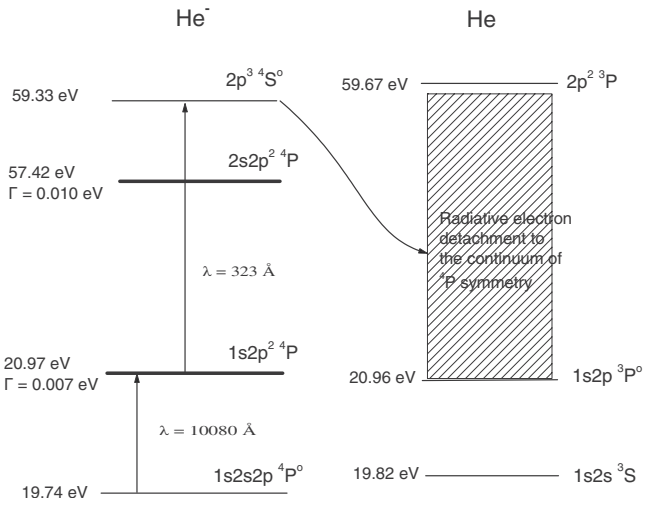

FIG. 1. Schematic representation of the quartet spectrum of He^- ($1s2s2p\,{}^4P^o$, $1s2p^2\,{}^4P$, and $2p^3\,{}^4S^o$) and of the corresponding triplet states of He. Energy levels, transitions, and radiationless widths.

The theoretical-computational task which we undertook dealt with the problem of determining from first principles the time-dependent probability of populating the triply excited $He^-\,2p^3\,{}^4S^o$ bound state, assuming that we start from the $1s2s2p\,{}^4P^o$ metastable state, and that we apply two weak electromagnetic pulses of $\lambda_1 = 10\,080$ Å and $\lambda_2 = 323$ Å having some delay (time overlap) between them. The induced, electric dipole-allowed evolution is

$$\mathrm{He}^-\,1s2s2p\,{}^4P^o \overset{1008\ \mathrm{nm}}{\rightarrow} |{}^4P(\varepsilon)\rangle \overset{32.3\ \mathrm{nm}}{\rightarrow} 2p^3\,{}^4S^o. \qquad (2)$$

$|{}^4P(\varepsilon)\rangle$ is the shape resonance that is labeled by the $1s2p^2\,{}^4P$ configuration. Its computation is done according to the state-specific theory of resonances discussed in our previous publications, e.g., [9]. Specifically, rather than following a scattering, close-coupling type calculation aiming at the determination of the energy-dependent phase shift, the emphasis is on determining separately the localized (square-integrable) and the asymptotic scattering components, which are then allowed to mix. The former consists of the Hartree-Fock (HF) $1s2p^2\,{}^4P$ wave function plus localized correlation among the three electrons. The latter consists of the $(1s2p\,{}^3P^o\varepsilon p\,{}^4P)$ energy-normalized scattering wave functions.

We note that in the above excitation sequence, the intermediate $1s2p^2\,{}^4P$ shape resonance may, in principle, be replaced by the $2s2p^2\,{}^4P$ resonance. However, the corresponding wavelengths and probability amplitudes are such that the field-induced excitation of the $2p^3\,{}^4S^o$ bound state is rendered less probable.

Finally, we refer to Fig. 1 in order to comment on the possible depletion channels of the target state, the $2p^3\,{}^4S^o$ bound state. There are two such main pathways. The first corresponds to spontaneous radiative electron detachment to the $(1s2p\,{}^3P^o\varepsilon p\,{}^4P + h\nu)$ scattering continuum. The second corresponds to the induced photodetachment $(2p^3\,{}^4S^o + h\nu \rightarrow \mathrm{He}\,2p^2\,{}^3P + \varepsilon\ell)$ by the soft x-ray pulse, with $\varepsilon \approx 38$ eV.

Other, higher-lying, photodetachment single and double ejection channels (e.g., He$2p3p\ ^3P+\varepsilon\ell$), have much smaller probability due to extremely small dipole matrix elements. The contribution of these two pathways was taken into account by using a complex energy for the $2p^3\ ^4S^o$ state, where the imaginary part is the sum of the half-widths that are caused by radiative autodetachment and by photodetachment. These widths (rates) were computed from first principles. Of the two, the one for radiative autodetachment (RA), $\Gamma_{RA}=1.38\times10^{-7}$ a.u. [9], is larger by orders of magnitude for the intensities that were used.

III. TWO THEORETICAL APPROACHES

A. State-specific function spaces

Both of the theoretical approaches that are described below are implemented using the same state-specific function spaces.

The square-integrable three-electron wave functions $\Phi_1(^4P^o)$, $\Phi_0(^4P)$, and $\Phi_2(^4S^o)$ correspond to the three states of the problem, $1s2s2p\ ^4P^o$, $1s2p^2\ ^4P$, and $2p^3\ ^4S^o$, while $U_\varepsilon(^4P)$ are energy-normalized scattering wave functions describing the states $He^-\ 1s2p\ ^3P^o\varepsilon p\ ^4P$. They are computed for a large number of values of the free electron energy, ε. A computationally convenient practice in the framework of the state-specific theory is for the scattering orbitals to be computed numerically in the single or multiconfigurational frozen HF potential of the $(N-1)$ electron state, accounting for the exchange integrals. In the present case, the situation is simple since the core is the $He1s2p\ ^3P^o$ state. The final calculation of the coupling matrix elements involving the $He^-\ 1s2p\ ^3P^o\varepsilon p\ ^4P$ basis completes the energy values via interpolation.

The state-specific bound wave functions were computed numerically as small multiconfigurational Hartree-Fock (MCHF) expansions using the code published by Froese-Fischer [20]. Provided the correct main configurations are included, such expansions not only are sufficiently accurate but also allow for physically transparent interpretations. The $\Phi_1(^4P^o)$ wave function for the $He^-\ 1s2s2p\ ^4P^o$ state consists of the initial numerical MCHF wave function $0.975(1s2s2p)-0.161(1s2p3d)$ and of eight additional correlation configurations containing variationally optimized virtual orbitals. Its energy is $E_1=-2.176\,623$ a.u. For the shape resonance, $\Phi_0(^4P)$, the calculated MCHF wave function is $0.900(1s2p^2)-0.423(1s3p^2)-0.104(1s3d^2)$, to which virtual excitations up to f orbitals were added. Its energy is $E_0=-2.131\,063$ a.u., i.e., 10.2 meV above the $He1s2p\ ^3P^o$ state. The experimental value is 10.8 meV [19]. Finally, the $\Phi_2(2p^3\ ^4S^o)$ state consists of the MCHF wave function $0.971(2p^3)-0.190(2p3p^2)-0.007(3p^3)+0.140(2p3d^2)$ and of three additional correlation configurations. The corresponding energy is $E_2=-0.720\,362$ a.u.

We stress that the above energies are given only for reasons of documentation and guidance. It is not the purpose of the SSEA calculations to obtain extremely accurate energies. For related discussions on the problem of electron correlation in ground and excited states as regards dominant effects and calculations to high order, the reader is referred to [21].

B. Solution of the TDSE to first order in perturbation theory: Recognition of the presence of terms contributing to nonexponential decay of the shape resonance

Let $H(t)$ be the time-dependent Hamiltonian describing the interaction between He^- (initially being in the $1s2s2p\ ^4P^o$ state) and two electromagnetic pulses. It is written as

$$H(t)=H^A+V^{(1)}(\omega_1,t)+V^{(2)}(\omega_2,t), \tag{3}$$

where H^A is the free-atom Hamiltonian and

$$V^{(i)}(\omega_i,t)=F_i g_i(t)\vec{e}_i\cdot\vec{r}\sin\omega_i(t-t_i),\quad i=1,2 \tag{4}$$

are the classical fields. F is the field strength, ω is the frequency, and $\vec{e}$ is the polarization vector. We define $T_i=\pi/\Omega_i$, where Ω_i is the angular frequency of the ramp-on and ramp-off parts of the pulses, which are assumed to have the general form

$$g_i(t)=\begin{cases}\sin^2\Omega_i(t-t_i), & t_i\le t\le t_i+T_i/2\\ 1, & t_i+T_i/2\le t\le t_i+t_c+T_i/2\\ \sin^2\Omega_i(t-t_c-t_i), & t_i+t_c+T_i/2\le t\le t_i+t_c+T_i.\end{cases} \tag{5}$$

Since we wish to apply perturbation theory to first order, the condition for its validity requires that the initial state time-dependent coefficient is very close to unity. This means that the interaction has to be weak as well as short. Hence for the first pulse, the time, t_C, during which the pulse is constant, is chosen equal to zero.

We use the symbols Φ_1 for the wave function of $He^-\ 1s2s2p\ ^4P^o$, Φ_2 for that of $He^-\ 2p^3\ ^4S^o$, and Ψ_E for the scattering states $He^-1s2p\varepsilon p\ ^4P$. The scattering states contain the shape resonance, whose localized part is symbolized by Φ_0 and is labeled by $He^-1s2p^2\ ^4P$. Its energy lies between E_1 and E_2, as it is shown in Fig. 1.

The total wave function $\Psi(t)$ is expanded in terms of eigenfunctions of H^A as

$$\Psi(t)=h_1(t)e^{-iE_1t}\Phi_1+h_2(t)e^{-iz_2t}\Phi_2+\int dE h_E(t)e^{-iEt}\Psi_E, \tag{6}$$

where $h_1(t)$, $h_2(t)$, and $h_E(t)$ are time-dependent amplitudes, $z_2=E_2-i\Gamma_{RA}$, and $E=E_{1s2p\ ^3P^o}+\varepsilon$. Ψ_E is defined in Eq. (11) and represents the mixing of Φ_0 and zero order scattering components.

$\Psi(t)$ is required to satisfy the TDSE ($\hbar=1$)

$$i\frac{\partial\Psi(t)}{\partial t}=H(t)\Psi(t). \tag{7}$$

There is no direct coupling between states 1 and 2 in the electric dipole approximation. Thus

$$\frac{dh_1}{dt}=-i\int dE h_E e^{-i(E-E_1)t}V_{1E}^{(1)}, \tag{8a}$$

$$\frac{dh_2}{dt} = -i\int dE h_E e^{-i(E-z_2)t} V_{2E}^{(2)}, \tag{8b}$$

$$\frac{dh_E}{dt} = -ih_1 e^{i(E-E_1)t} V_{1E}^{(1)} - ih_2 e^{i(E-z_2)t} V_{2E}^{(2)}, \tag{8c}$$

where $V_{iE}^{(j)}$ are the matrix elements coupling the bound states $|\Phi_i\rangle$ to the continuum of $|\Psi_E\rangle$.

We are interested in the amplitude h_2 as a function of the time at which the second pulse starts its interaction. The hallmark of perturbation theory is the assumption that for the interaction period, $h_1 \approx 1$ and $h_2 \approx 0$. Thus to first order,

$$h_E(t) \approx -i\int_0^t dt' e^{i(E-E_1)t'} V_{1E}^{(1)}(t'). \tag{9}$$

Substituting Eq. (9) into Eq. (8) and changing the order of the E and t' integrations, we obtain

$$h_2(t_{\text{delay}}) \approx -\int_{t_2}^{T_2} dt e^{iz_2 t} \int_{t_1}^{t} dt' e^{-iE_1 t'} \times \int dE e^{-iE(t-t')} V_{1E}^{(1)}(t') V_{2E}^{(2)}(t), \tag{10}$$

where $t_{\text{delay}} = t_2 - t_1$. Note that $t' \le t$ in the above formula.

Further progress requires specifying the functional forms of the matrix elements that couple the bound states to the energy continuum. To this end, we make use of the Fano form of a resonance as a superposition of the square integrable Φ_0 and the continuum of scattering states U_E, with normalization $\langle U_E | U_{E'} \rangle = \delta(E-E')$. We subject the shape resonance to the same formalism, meaning that we emphasize the separation of the full space into a localized part and a scattering part. However, in the case of a shape resonance the formalism has to be adapted to the fact that, in practice, this separation leads to overlaps, $S_{0E} = \langle \Phi_0 | U_E \rangle$. Thus denoting with P the principal value integrations, the form of the Fano superposition is

$$\Psi_E = a_E \left[\Phi_0 + P\int dE' U_{E'} \frac{1}{E-E'} W_{E'0}(E) + U_E \frac{E - E_0 - \Delta(E)}{W_{E0}(E)} \right], \tag{11}$$

where the interaction matrix elements are

$$W_{0E'}(E) = V_{0E'} - ES_{0E'}. \tag{12}$$

We note that for negative ions the integrals $V_{0E'}$ and $S_{0E'}$ are relatively large numbers which nearly cancel each other, giving values for W at the appropriate order of magnitude.

The energy dependent coefficient a_E is given by

$$a_E = \left[\frac{1}{\pi} \frac{\Gamma(E)}{[E - E_0 - \Delta(E)]^2 + \Gamma^2(E)} \right]^{1/2}, \tag{13}$$

where the half-width function

$$\Gamma(E) = \pi W_{0E}^2(E) \tag{14}$$

and the energy shift function

$$\Delta(E) = P\int dE' \frac{W_{0E'}^2(E)}{E - E'} \tag{15}$$

are, for the case of the He^- $1s2p^2\ ^4P$ shape resonance, strongly energy dependent.

The calculation of the electric dipole matrix elements $D_{iE} = \langle \Phi_i | \vec{D} | U_E \rangle$ shows that they are negligible in comparison to the matrix elements connecting bound states $D_{i0} = \langle \Phi_i | \vec{D} | \Phi_0 \rangle$. Therefore only the contribution of the bound part of Eq. (11) needs to be taken into account. Thus

$$V_{iE}^{(i)}(t) = a_E F_i D_{i0} g_i(t) \sin \omega_i (t - t_i) \tag{16}$$

and the energy dependence of the matrix element results solely from the coefficient a_E. Substitution of the form (16) in Eq. (10) with $t_1 = 0$ and $t_2 = t_{\text{delay}}$ gives

$$h_2(t_{\text{delay}}) \approx -F_1 F_2 D_{10} D_{20} \int_{t_{\text{delay}}}^{T_2} dt e^{iz_2 t} g_2(t) \times \sin \omega_2 (t - t_{\text{delay}}) \int_0^t dt' e^{-iE_1 t'} g_1(t') \sin \omega_1 t' \frac{1}{\pi} \times \int_0^\infty dE \frac{\Gamma(E) e^{-iE(t-t')}}{[E - E_0 - \Delta(E)]^2 + \Gamma^2(E)}. \tag{17}$$

We perform the energy integration first, taking into account the $t' \le t$ condition. The method, described in Appendix A, produces the result

$$b e^{-iz_0 \delta t} - \frac{1}{2\pi i} \sum_i b_i \{ e^{-iz_{0i}\delta t} \mathrm{E}_1[i(E_i - z_{0i})\delta t] - e^{-iz_{0i}\delta t} \mathrm{E}_1[i(E_{i+1} - z_{0i})\delta t] \} + \frac{1}{2\pi i} \times \sum_i b_i^* \{ e^{-iz_{0i}^* \delta t} \mathrm{E}_1[i(E_i - z_{0i}^*)\delta t] - e^{-iz_{0i}^* \delta t} \mathrm{E}_1[i(E_{i+1} - z_{0i}^*)\delta t] \}. \tag{18}$$

The summation in Eq. (18) is over an energy mesh of points $\{E_i\}$. $\delta t = t - t'$, and $\mathrm{E}_1(z)$ is defined in Appendix B. The coefficients are given by

$$b_i = \frac{1}{1 - \Delta_i' + i\Gamma_i'}, \tag{19}$$

where the prime signifies the derivative with respect to energy.

The true pole z_0 in the expression (17) is the particular value z_{i0} for which $E_i < E_0 + \tilde{\Delta}_i < E_{i+1}$, and b is the corresponding value of b_i. The modified quantities $\tilde{\Gamma}$ and $\tilde{\Delta}$, which are defined in Eq. (A7), depend on Δ, Δ', Γ, and Γ'.

Equation (18) is related to the intrinsic time-dependent properties of the formation and decay of the nonstationary shape resonance. Specifically, it contains the corrections to its exponential decay that are due to the energy dependence of the width and shift functions, as well as to the fact that the energy integration is constrained to start from zero and not from minus infinity. Thus the exponentially decaying term in

Eq. (18), $e^{-iz_0\delta t}$, is multiplied by a factor greater than unity, ($|b| \approx 1.53$), which is caused by the energy-dependence of the resonance parameters. Its effect is equivalent to starting in Eq. (17) with an asymmetric Breit-Wigner form $\pi^{-1}\frac{\mathrm{Re}\, b\tilde{\Gamma} - \mathrm{Im}\, b(E-E_0-\tilde{\Delta})}{(E-E_0-\tilde{\Delta})^2+\tilde{\Gamma}^2}$ instead of a Lorentzian form with constant width and shift. Additionally, there is also the nonexponential decay contribution that is represented in terms of the exponential integral function, $\mathrm{E}_1(z)$ [22].

The next step in the determination of h_2 is to perform the time integrations. Since the first pulse interacts in the time interval $[0, T_1]$, the first time integration is split into an integral with $t' < T_1$ and an integral with $t' > T_1$. The second time integration is performed for each of the above integrals separately.

Since the second pulse interacts in the time interval $[t_{\mathrm{delay}}, t_c + T_2]$, the form of the integrals depends on which of the three conditions is met:

(i) $t_{\mathrm{delay}} + t_c + T_2 < T_1$, i.e., the two pulses act simultaneously.

(ii) $t_{\mathrm{delay}} < T_1 < t_{\mathrm{delay}} + t_c + T_2$, i.e., the second pulse continues to act after the first has stopped.

(iii) $T_1 < t_{\mathrm{delay}}$, i.e., both pulses act independently.

The integrals involving the simple exponential of the first term are trivial. Those involving the E_1 functions are given in Appendix B. In the final evaluation, a routine for $\mathrm{Ei}(z)$ from the "Numerical Recipes" of Press *et al.* [23], converted to complex values, has been employed.

The matrix elements that are required for the implementation of the present theory are obtained with state-specific wave functions that were described in the previous section.

C. Nonperturbative solution of the TDSE by the SSEA

We now turn to the *ab initio*, nonperturbative, numerical solution of the TDSE by the SSEA. For the problem described in Eq. (2), for linear polarization and the electric dipole approximation, the time-dependent Hamiltonian is given by Eqs. (3)–(5).

The first point that must be made is that, given the symmetries of the states and the electric dipole selection rules, the polarizations of the pulses were chosen to be perpendicular. Specifically, since the total angular momentum of $2p^3\,{}^4S^o$ is 0 and that of the intermediate state, $1s2p^2\,{}^4P$, is 1, the allowed dipole transitions are restricted between states with total magnetic quantum numbers $\mathrm{M}=0$ for $2p^3\,{}^4S^o$ and $\mathrm{M} = \pm 1$ for $1s2p^2\,{}^4P$. Therefore a computationally economic and experimentally realistic excitation scheme is the following: First, the initial state is prepared in its $\mathrm{M}=1$ component and the transition occurs to the $\mathrm{M}=1$ component of the intermediate state by a linearly polarized laser pulse along the z axis, $zF_1g_1(t)\sin(\omega_1 t)$. Then, after a time-delay t_{delay}, the interaction with the second pulse, which is polarized along the x axis, $xF_2g_2(t-t_{\mathrm{delay}})\sin[\omega_2(t-t_{\mathrm{delay}})]$, causes the time-dependent transition to the final state, $2p^3\,{}^4S^o$.

According to the main idea of the SSEA, the $\Psi_{\mathrm{SSEA}}(t)$ for this problem is the time-dependent superposition of state-specific wave functions,

$$\Psi_{\mathrm{SSEA}}(t) = c_1(t)\Phi_1({}^4P^o) + c_0(t)\Phi_0({}^4P) + c_2(t)\Phi_2({}^4S^o) + \int_0 d\varepsilon c_\varepsilon(t) U_\varepsilon({}^4P). \tag{20}$$

In comparing expansions (6) and (20), the coefficients $c_1(t)$ and $c_2(t)$ are equal to the corresponding $h_1(t)$ and $h_2(t)$, while the relation of $c_0(t)$ and $c_\varepsilon(t)$ to $h_E(t)$ is given in Ref. [24].

Substitution of Eq. (20) into the TDSEs (3) and (7) transforms it into the following system of coupled integrodifferential equations with time-dependent coefficients:

$$i\frac{dc_1(t)}{dt} = E_1c_1(t) + D_{10}F_1g_1(t)\sin\omega_1 t c_0(t) + F_1g_1(t)\sin\omega_1 t \int d\varepsilon D_{1\varepsilon}c_\varepsilon(t), \tag{21a}$$

$$i\frac{dc_0(t)}{dt} + i\int d\varepsilon S_{0\varepsilon}\frac{dc_\varepsilon(t)}{dt} = E_0c_0(t) + \int d\varepsilon V_{0\varepsilon}c_\varepsilon(t) + D_{10}F_1g_1(t)\sin(\omega_1 t)c_1(t) + F_2g_2(t-t_{\mathrm{delay}})\sin[\omega_2(t-t_{\mathrm{delay}})]D_{20}c_2(t), \tag{21b}$$

$$i\frac{dc_\varepsilon(t)}{dt} + iS_{0\varepsilon}\frac{dc_0(t)}{dt} = (E_{1s2p\ {}^3P^o} + \varepsilon)c_\varepsilon(t) + V_{0\varepsilon}c_0(t) + \mathrm{D}_{1\varepsilon}F_1g_1(t)\sin\omega_1 t c_1(t) + F_2g_2(t-t_{\mathrm{delay}})\sin\omega_2(t-t_{\mathrm{delay}})D_{2\varepsilon}c_2(t), \tag{21c}$$

$$i\frac{dc_2(t)}{dt} = (E_2 - i\Gamma_{RA})c_2(t) + F_2g_2(t-t_{\mathrm{delay}}) \times \sin\omega_2(t-t_{\mathrm{delay}})D_{20}c_0(t) + F_2g_2(t-t_{\mathrm{delay}}) \times \sin\omega_2(t-t_{\mathrm{delay}}) \int d\varepsilon D_{2\varepsilon}c_\varepsilon(t). \tag{21d}$$

The initial condition at $t=0$ is $V^{(1)}(\omega,0)=0$ and $c_1(0)=1$. As soon as $t>0$, the relevant configurations are mixed via $H(t)$, while $t > t_{\mathrm{delay}}$ starts the population transfer to the $\mathrm{He}^-\ 2p^3\,{}^4S^o$ state. The quantities,

$$D_{10} = \langle\Phi_1({}^4P^o)|z|\Phi_0({}^4P)\rangle,$$

$$D_{1\varepsilon} = \langle\Phi_1({}^4P^o)|z|U_\varepsilon({}^3P^o\varepsilon p\,{}^4P)\rangle,$$

$$S_{0\varepsilon} = \langle\Phi_0({}^4P)|U_\varepsilon({}^3P^o\varepsilon p\ {}^4P)\rangle,$$

$$V_{0\varepsilon} = \langle\Phi_0({}^4P)|H^A|U_\varepsilon({}^3P^o\varepsilon p\ {}^4P)\rangle,$$

$$D_{20} = \langle\Phi_2({}^4S^o)|x|\Phi_0({}^4P)\rangle,$$

$$D_{2\varepsilon} = \langle\Phi_2({}^4S^o)|x|U_\varepsilon({}^3P^o\varepsilon p\ {}^4P)\rangle, \quad \Gamma_{RA} = 1.38\times10^{-7}\ \text{a.u.}$$

are computed numerically. The coupling matrix elements resulting from the integral over the continuum are constructed

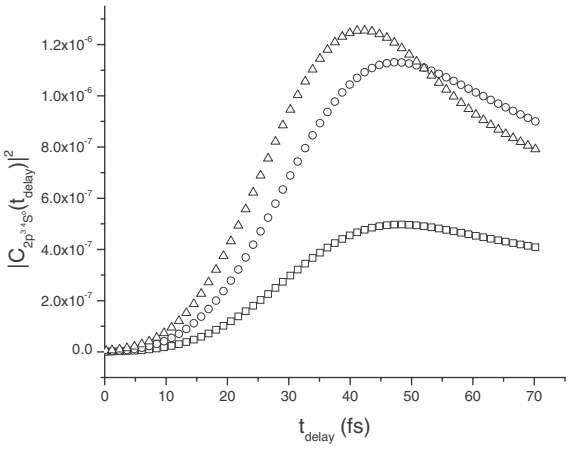

FIG. 2. Probability of populating the $He^- 2p^3\ ^4S^o$ state, at the end of the second pulse, as a function of t_{delay} between the two pulses for $t_C=0$ [see Eq. (5)]. The durations are 67 fs (20 cycles) for the first (pump) pulse and 22 fs (200 cycles) for the second one. The corresponding wavelengths are $\lambda_1=10\,080$ Å and $\lambda_2=323$ Å with peak field strengths $F_1=5\times10^{-5}$ a.u. and $F_2=5\times10^{-4}$ a.u. Rectangles: results from the three-state model system (see text). Circles: results based on the use of just the first term of Eq. (18). Triangles: results based on the full Eq. (18) and on the nonperturbative numerical integration of the system (21).

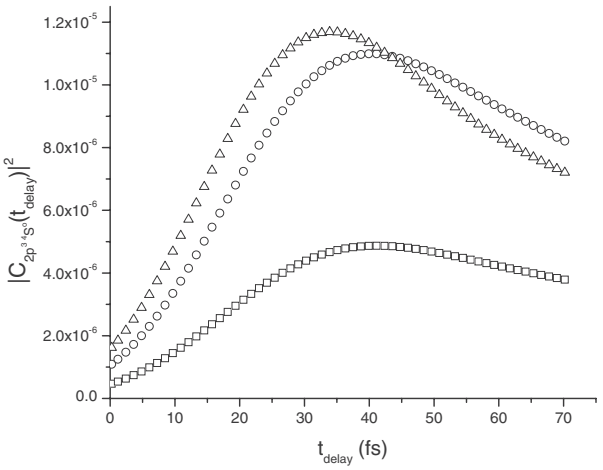

FIG. 3. As in Fig. 2, but for a longer second pulse, with $t_C=24$ fs and duration 46 fs.

as accurately as is necessary by extending the energy range and by increasing the density of energy points via direct computation and interpolation.

Finally, the propagation of $\Psi_{SSEA}(t)$ in time, i.e., the calculation of the time-dependent coefficients, is done by the Taylor-series expansion method described in [2], which was appropriately modified to handle the overlap, $S_{0\varepsilon}$, between the nonorthonormal basis sets describing the localized part of the shape resonance $\Phi_0(1s2p^2\ ^4P)$ and the underlying continuum $U_\varepsilon(1s2p\ ^3P^o\varepsilon p\ ^4P)$.

The final results were obtained from the solution of Eqs. (21) with about 20 000 terms, for a range of energy, ε, from 0 to 1.0 a.u. The wavelengths of the two pulses are given in Eq. (2). For reasons given below, a number of values for the durations of the two pulses were combined. This was done by varying the constant portion of the pulse, t_c. When $t_c=0$, the durations are 67 fs (20 cycles) for the first (pump) pulse and 22 fs (200 cycles) for the second one.

IV. RESULTS

The results from the perturbative and the nonperturbative calculations are presented in Figs. 2 and 3 and in Table I. We stress that the two field strengths are weak: $F_1=5\times10^{-5}$ a.u. and $F_2=5\times10^{-4}$ a.u.

In Fig. 2, we show the probability of populating the $\Phi_2(2p^3\ ^4S^o)$ state, $|C_{2p^3\ ^4S^o}(t_{\text{delay}})|^2$, as a function of t_{delay} between the two pulses for $t_C=0$, for three sets of calculations that are based on Eq. (18) as well as on the numerical solution of the TDSE by the SSEA. The latter provides the accurate reference results, which are in complete agreement with those obtained when the full Eq. (18) is used.

The first set of results are based on a model system consisting of the three states, $\Phi_1(1s2s2p\ ^4P^o)$, $\Phi_0(1s2p^2\ ^4P)$, and $\Phi_2(2p^3\ ^4S^o)$, without the explicit contribution of the free electron continuum represented by the basis $U_\varepsilon(1s2p\ ^3P^o\varepsilon p\ ^4P)$. The effects of discrete-scattering state interaction defining the shape resonance are incorporated approximately by adding an imaginary part, Γ_0, to the energy, E_0, of $\Phi_0(1s2p^2\ ^4P)$. Γ_0 is assigned the experimental value for the half-width, 3.58 meV [19]. In decaying state theory, the assumption of a constant decay width produces a Lorentzian distribution and, in turn, if the energy integration goes from minus to plus infinity, exponential decay. The maximum value for $|C_{2p^3\ ^4S^o}(t_{\text{delay}})|^2$ is 5×10^{-7} and occurs for $t_{\text{delay}}=48$ fs.

The second set of results are based on the use of just the first term of Eq. (18). Now, the energy-dependent coefficient [Eq. (19)] causes deviation from a pure exponential decay of the $\Phi_0(1s2p^2\ ^4P)$ state for all times. This is due to the fact that, for this shape resonance, $\Gamma(E)$ and $\Delta(E)$ are strongly

TABLE I. Variation of the probability of populating the $He^- 2p^3\ ^4S^o$ state as a function of the duration of the two pulses, using $t_{\text{delay}}=44$ fs. The other parameters are as in Fig. 2. Differences up to four orders of magnitude are observed.

$\lvert C_{2p^3\ ^4S^o}\rvert^2$	First pulse ($\lambda_1=10\,080$ Å) duration (fs)	Second pulse ($\lambda_2=323$ Å) duration (fs)
1.2×10^{-6}	67 ($t_c=0$ fs)	22 ($t_c=0$ fs)
1.4×10^{-4}	67 ($t_c=0$ fs)	215 ($t_c=193$ fs)
2.2×10^{-4}	67 ($t_c=0$ fs)	457 ($t_c=435$ fs)
7.1×10^{-4}	91 ($t_c=24$ fs)	457($t_c=435$ fs)
1.9×10^{-6}	357 ($t_c=290$ fs)	22 ($t_c=0$ fs)
6.1×10^{-4}	357 ($t_c=290$ fs)	118 ($t_c=96$ fs)
3.6×10^{-3}	357 ($t_c=290$ fs)	215 ($t_c=193$ fs)
1.0×10^{-2}	357 ($t_c=290$ fs)	312 ($t_c=290$ fs)
1.8×10^{-2}	357 ($t_c=290$ fs)	457 ($t_c=435$ fs)

energy dependent. The maximum value for $|C_{2p^3\,^4S^o}(t_{\text{delay}})|^2$ is 1.1×10^{-6} and occurs for $t_{\text{delay}}=47$ fs.

The third set of results are based on the full Eq. (18) and are verified by the independent numerical solution of the TDSE via the SSEA, for the weak field strengths $F_1=5\times10^{-5}$ a.u. and $F_2=5\times10^{-4}$ a.u. In the latter case, both bound and scattering state-specific components are part of the wave function superposition. As time integration proceeds, each component contributes to the evolution of the system. The final result contains information that is connected to both exponential and nonexponential decay of the initially localized shape resonance, $\Phi_0(1s2p^2\,^4P)$.

In the former case, these two types of decay are represented explicitly by the expression (18). The maximum in the accurate results is 1.3×10^{-6} and occurs for $t_{\text{delay}}=42$ fs. Hence the maximum is shifted to smaller values of t_{delay} and the shape of the curve becomes sharper.

The corresponding main conclusions are the following.

(1) The effect of the pump-probe time delay as a control parameter is demonstrated quantitatively for a multiply excited spectrum inside the continuous spectrum of a polyelectronic system (an atomic negative ion).

(2) The terms in expression (18) that have been identified as originating from the nonexponential decay of the intermediate resonance state have a clear effect on the time-dependent occupation probability of the target state. Therefore we conclude that for time delays such as those used here, it is possible to distinguish the deviation from the exponential decay model that is associated with the Lorentzian distribution with constant width and with energy integration starting from $-\infty$.

In Fig. 3 and in Table I we present a selected set of results of SSEA computations whose purpose was to explore and to understand quantitatively how the time-dependent occupation probability of the target state changes as a function of the duration of the two pulses for a fixed value of the time-delay in the region where the efficiency of the process is maximum.

For these calculations we took account of the fact that in the photoabsorption experiment of Walter, Seifert, and Peterson [19], the excitation $\text{He}^-1s2s2p\,^4P^o \xrightarrow{1008\ \text{nm}} |^4P(\varepsilon)\rangle$ was achieved by essentially cw radiation. This suggests that the pump pulse can be taken to be relatively long, a fact that increases the probability of the overall transition to the $\Phi_2(2p^3\,^4S^o)$ state. A simple way to vary the pulse duration is to maintain the rise and off times equal to $T_2/2$ and to increase the time t_C where the field strength is constant. [See Eq. (5)].

In Fig. 3, we show the same quantities as in Fig. 2. However, now for the second pulse we assume $t_C>0$. As t_C increases, the probability of populating the $\Phi_2(2p^3\,^4S^o)$ state acquires values by an order of magnitude larger than those in Fig. 2. In addition, the maxima of the three sets of results are shifted to smaller values of t_{delay} and the shapes of the curves broaden. Specifically, corresponding to the three cases mentioned above, the results show the following. For the model calculation, the maximum value for $|C_{2p^3\,^4S^o}(t_{\text{delay}})|^2$ is 4.9×10^{-6} and occurs for $t_{\text{delay}}=41$ fs. For the case where only the first term of Eq. (18) is accounted for, the maximum value for $|C_{2p^3\,^4S^o}(t_{\text{delay}})|^2$ is 1.1×10^{-5} and occurs for $t_{\text{delay}}=41$ fs. For the exact calculation, the maximum value for $|C_{2p^3\,^4S^o}(t_{\text{delay}})|^2$ is 1.2×10^{-5} and occurs for $t_{\text{delay}}=34$ fs.

It should be noted that the results corresponding to the first term of Eq. (18), which represents an exponential decay of the $\Phi_0(1s2p^2\,^4P)$ state where the energy dependence of the parameters $\Gamma(E)$, $\Delta(E)$ is taken into account, approach the accurate ones.

Finally, for the sake of completeness, we performed calculations that exhibit the dependence of the efficiency of reaction (2) on the duration of both pulses, in the case where $t_C>0$. In this case, the fact that the first pulse is long implies that the first-order perturbative treatment breaks down, since the initial state coefficient becomes smaller than unity [see discussion before Eq. (9)]. Therefore the question had to be answered via the SSEA solution of the system of integrodifferential equations (21). The results are shown in Table I.

As an example we refer here to two sets of results: When the first pulse lasts for 67 fs and the second 22 fs, i.e., when t_C is zero for both, the occupation probability of $|2p^3\,^4S^o\rangle$ is 1.2×10^{-6}, which is very small. However, this increases by almost four orders of magnitude (1.8×10^{-2}) when the first pulse lasts for 357 fs and the second one for 457 fs.

V. CONCLUSIONS

The theory and results that were described in the previous sections combined notions and theoretical methods from different areas of modern atomic physics in order to compute time-resolved observable quantities in the scale of a few tens of femtoseconds, by solving from first principles a prototypical TDMEP.

Specifically, we considered the interaction of two weak monochromatic electromagnetic pulses, having a variable time delay in the range of 0–73 fs, with the metastable state of the three-electron atomic negative ion, $\text{He}^-\,1s2s2p\,^4P^o$. The duration of each of the two pulses was allowed to vary in the range from 67 to 460 fs, and their wavelengths were fixed on the energy differences $E(1s2s2p\,^4P^o)-E(1s2p^2\,^4P)$, $\lambda=10\,080$ Å, and $E(1s2p^2\,^4P)-\text{E}(2p^3\,^4S^o)$, $\lambda=323$ Å. The states labeled by $1s2s2p\,^4P^o$ and $2p^3\,^4S^o$ are discrete but the one labeled by $1s2p^2\,^4P$ is an energy dependent shape resonance. There is an underlying continuum of scattering states, whose basis is labeled by $1s2p\,^3P^o\varepsilon p\,^4P$, where ε is the free electron energy.

The question is how the three electrons respond and how the system evolves in time while the target state, the triply excited bound state, $\text{He}^-\,2p^3\,^4S^o$, is being populated as a function of time. The problem was solved and analyzed via two approaches. In the first, we employed time-dependent perturbation theory to first order and obtained analytic solutions, in which the quantities are computed in terms of state-specific correlated wave functions. In the second, the TDSE was solved nonperturbatively by applying the SSEA. We note that the first implementation of the SSEA was also on a TDMEP that involved an atomic negative ion, the Li^- [2].

The quantitative results give for the first time an idea of the order of magnitude for the time-dependent probabilities

of such processes. Specifically, they show how the probability of producing $He^- 2p^3\,{}^4S^o$ via the continuous spectrum where a shape resonance ($1s2p^2\,{}^4P$) is present varies as a function of the time delay, t_{delay}, between the two electromagnetic short pulses. Hence t_{delay} in this problem constitutes a practical control parameter for the efficiency of reaction (2). In fact, this efficiency increases when the duration of the two pulses increases.

Finally, we showed that by monitoring the time-dependent population of the target state, $He^- 2p^3\,{}^4S^o$, as a function of t_{delay}, it is possible to draw conclusions as to the indirect effect of short-time deviations from exponential decay of a shape resonance with a strong energy dependence. The prospects of implementing novel spectroscopic techniques currently being developed for detecting the effects of electronic motion at the attosecond scale, e.g. [25], should probably include this possibility.

ACKNOWLEDGMENTS

This work was partially supported by the program "Pythagoras," which is co-funded by the European social fund (75%) and national resources (25%). It was also partially supported by the program "Karatheodori" of the National Technical University, Athens, Greece.

APPENDIX A

We describe a method for the calculation of the energy integral in Eq. (17) with great precision, while E remains on the real axis. We start by assuming that $\Gamma(E)$ and $\Delta(E)$ are constants. The integration of the resulting Lorentzian distribution is then easy. Specifically, after analyzing it into partial fractions as

$$\frac{\Gamma}{(E-E_0-\Delta)^2+\Gamma^2}=\frac{1}{2i}\left[\frac{1}{E-z_0^*}-\frac{1}{E-z_0}\right], \tag{A1}$$

where

$$z_0=E_0+\Delta-i\Gamma, \tag{A2}$$

the integrations produce well-known functions, i.e.,

$$\int_{E_a}^{E_b} dE\frac{e^{-iEt}}{E-z_0}=-2\pi i\theta(E_b-\mathrm{Re}\,z_0)\theta(\mathrm{Re}\,z_0-E_a)e^{-iz_0t} + e^{-iz_0t}\mathrm{E}_1[i(E_a-z_0)t]-e^{-iz_0t}\mathrm{E}_1[i(E_b-z_0)t], \tag{A3}$$

where $\theta(x)$ is the step function and $\mathrm{E}_1(z)=\int_z^\infty dx\frac{e^{-x}}{x}$ (see Appendix B). The latter is an analytic function in the z plane cut along the negative real axis. The first term in Eq. (A3), which is the contribution of the pole in contour integration calculations, results from the crossing of the brunch cut. Such a term is absent in the corresponding integration involving the pole z_0^* where the integration path crosses the positive real axis.

In order to take into account the energy variation of $\Gamma(E)$ and $\Delta(E)$, we create an energy mesh of points $\{E_i\}$. Within each interval $[E_i,E_{i+1}]$ the functions are assumed to vary linearly as

$$\Delta(E)=\Delta_i+\Delta_i'(E-E_i), \tag{A4}$$

$$\Gamma(E)=\Gamma_i+\Gamma_i'(E-E_i), \tag{A5}$$

and so the denominators on the right-hand side of Eq. (A1) become

$$E-E_0-\Delta(E)\pm i\Gamma(E)=(1-\Delta'\pm i\Gamma_i')(E-E_0-\tilde{\Delta}_i\pm i\tilde{\Gamma}_i), \tag{A6}$$

where

$$\tilde{\Delta}_i\mp i\tilde{\Gamma}_i=\frac{\Delta(E_0)\mp i\Gamma(E_0)}{1-\Delta_i'\pm i\Gamma_i'}. \tag{A7}$$

The functions in the numerator of Eqs. (A7) are evaluated from Eqs. (A4) and (A5), and hence they are interval-dependent. Furthermore, a different value of the "pole" exists within each interval

$$z_{0i}=E_0+\tilde{\Delta}_i-i\tilde{\Gamma}_i. \tag{A8}$$

Implementation of this approach in the energy integration of Eq. (15) in conjunction with the rotating wave approximation gives the desired result, Eq. (18).

APPENDIX B

The function $\mathrm{E}_1(z)$

$$\mathrm{E}_1(z)=\int_z^\infty dx\frac{e^{-x}}{x} \tag{B1}$$

is defined in the complex z plane cut along the negative real axis. It has the series expansion

$$\mathrm{E}_1(z)=-\gamma-\ln z-\sum_{n=1}^{\infty}\frac{(-1)^n z^n}{nn!},\quad |\arg z|<\pi, \tag{B2}$$

where γ is the Euler constant, 0.577 21…. From the definition (B1) it follows that

$$\frac{d\mathrm{E}_1(z)}{dz}=-\frac{e^{-z}}{z}. \tag{B3}$$

This expression is used for the calculation of integrals involving $\mathrm{E}_1(z)$. The following integral has been used for the evaluation of the time integrations:

$$\int_{t_1}^{t_2} dte^{-i(a-b)t}\,\mathrm{E}_1[i(E-a)t] = \frac{i}{a-b}\{e^{-i(a-b)t_2}\,\mathrm{E}_1[i(E-a)t_2]-e^{-i(a-b)t_1}\,\mathrm{E}_1[i(E-a)t_1] - \mathrm{E}_1[i(E-b)t_2]+\mathrm{E}_1[i(E-b)t_1]\}. \tag{B4}$$

In the case $t_1\to 0$, the expansion (B2) is used for the replacement of the pair of $\mathrm{E}_1(z)$ functions by logarithms.

[1] K. Bergmann, H. Theuer, and B. W. Shore, Rev. Mod. Phys. **70**, 1003 (1998).
[2] Th. Mercouris, Y. Komninos, S. Dionissopoulou, and C. A. Nicolaides, Phys. Rev. A **50**, 4109 (1994).
[3] Th. Mercouris, I. D. Petsalakis, and C. A. Nicolaides, Chem. Phys. Lett. **208**, 197 (1993); C. A. Nicolaides, Th. Mercouris, and I. D. Petsalakis, *ibid.* **212**, 685 (1993); I. D. Petsalakis, Th. Mercouris, and C. A. Nicolaides, Chem. Phys. **189**, 615 (1994).
[4] T. Andersen, Phys. Rep. **394**, 157 (2004).
[5] G. J. Schulz, Rev. Mod. Phys. **45**, 378 (1973); S. J. Buckman and C. W. Clark, *ibid.* **66**, 539 (1994).
[6] C. A. Nicolaides, G. Aspromallis, and D. R. Beck, J. Mol. Struct.: THEOCHEM **199**, 283 (1989).
[7] N. A. Piangos and C. A. Nicolaides, J. Phys. B **31**, L147 (1998).
[8] D. R. Beck and C. A. Nicolaides, Chem. Phys. Lett. **59**, 525 (1978).
[9] (a) C. A. Nicolaides, Y. Komninos, and D. R. Beck, Phys. Rev. A **24**, 1103 (1981); (b) C. A. Nicolaides and Y. Komninos, Chem. Phys. Lett. **80**, 463 (1981).
[10] J. W. Hiby, Ann. Phys. **34**, 473 (1939).
[11] E. Holøien and J. Midtdal, Proc. Phys. Soc., London, Sect. A **68**, 815 (1955).
[12] I. M. Blau, R. Novick, and D. Weinflash, Phys. Rev. Lett. **24**, 1268 (1970).
[13] M. Agentoft, T. Andersen, and K. T. Chung, J. Phys. B **17**, L433 (1984); E. Träbert, P. H. Heckmann, J. Doerfert, and J. Granzow, *ibid.* **25**, L353 (1992); E. J. Knystautas, Phys. Rev. Lett. **69**, 2635 (1992).
[14] M. Bylicki and G. Pestka, J. Phys. B **29**, L353 (1996).
[15] J. L. Tech and J. F. Ward, Phys. Rev. Lett. **27**, 367 (1971); K. Aashamar, Nucl. Instrum. Methods **90**, 263 (1970).
[16] M. Bylicki and C. A. Nicolaides, Phys. Rev. A **48**, 3589 (1993).
[17] R. C. Bilodeau, J. D. Bozek, A. Aguilar, G. D. Ackerman, G. Turri, and N. Berrah, Phys. Rev. Lett. **93**, 193001 (2004).
[18] A. U. Hazi and K. Reed, Phys. Rev. A **24**, 2269 (1981).
[19] C. W. Walter, J. A. Seifert, and J. R. Peterson, Phys. Rev. A **50**, 2257 (1994).
[20] C. Froese-Fischer, Comput. Phys. Commun. **14**, 145 (1978).
[21] C. A. Nicolaides, Int. J. Quantum Chem. **102**, 250 (2005), and references therein.
[22] For analysis and calculations from first principles of nonexponential decay in real, polyelectronic nonstationary atomic states, see C. A. Nicolaides and Th. Mercouris, J. Phys. B **29**, 1151 (1996); Th. Mercouris and C. A. Nicolaides, *ibid.* **30**, 811 (1997); C. A. Nicolaides, Phys. Rev. A **66**, 022118 (2002).
[23] H. W. Press, S. A. Teukolsky, W. T. Vetterling, and B. P. Flannery, *Numerical Recipes* (Cambridge University Press, Cambridge, England 1992).
[24] Th. Mercouris, Y. Komninos, and C. A. Nicolaides, Phys. Rev. A **75**, 013407 (2007).
[25] P. H. Bucksbaum, Science **317**, 766 (2007).